

**( $n-2$ )-fold resonant splitting in open periodic quantum structures**Yuan Ping Chen,<sup>1</sup> Yue E. Xie,<sup>1</sup> and Xiao Hong Yan<sup>2</sup><sup>1</sup>*Institute of Modern Physics and Department of Physics, Xiangtan University, Xiangtan 411105, China*<sup>2</sup>*College of Science, Nanjing University of Aeronautics and Astronautics, Nanjing 210016, China*

(Received 22 January 2006; revised manuscript received 29 May 2006; published 12 July 2006)

We have calculated the conductance for two kinds of open periodic structures, using the lattice Green's function method. It is found that ( $n-2$ )-fold resonant splitting appears at energies slightly higher than the first threshold energy, while resonant peaks satisfying the ( $n-1$ )-fold splitting rule exist in the low-energy region of the conductance profile. The ( $n-2$ )-fold resonant splitting peaks are induced by high quasibound states in which electrons are mainly localized in the constrictions rather than in the stubs or junctions of the open structures. To this kind of quasibound state, the stub or junction acts as a potential barrier rather than a well, which is the inverse of the case of the quasibound states corresponding to the ( $n-1$ )-fold splitting peaks. It is also found that the number of high quasibound states existing in each constriction is related to the constriction length. In order to observe the ( $n-2$ )-fold resonant splitting, the constrictions between stubs or junctions in the open structure should be sufficiently long.

DOI: [10.1103/PhysRevB.74.035310](https://doi.org/10.1103/PhysRevB.74.035310)

PACS number(s): 73.21.-b, 85.35.Be

**I. INTRODUCTION**

Technological advances in microfabrication techniques now allow the manufacture of various kinds of low-dimensional periodic quantum structures.<sup>1-5</sup> Superlattices, as typical periodic quantum structures, have attracted considerable attention from both theoretical and experimental researchers, due to the importance of understanding the physics of quantum phenomena and their great technological potential.<sup>6-10</sup> It is well known that, for an electric or magnetic superlattice consisting of  $n$  identical potential or magnetic barriers, ( $n-1$ )-fold resonant splitting exists in the conductance as a function of electron energy.<sup>7,10</sup> These resonant splitting peaks correspond to the quantum bound states whose wave functions are localized in the wells. While the ( $n-1$ )-fold resonant peak splitting rule is also found in the open periodic structure,<sup>11-14</sup> in an open periodic structure such as a periodic multiwaveguide structure, there are no potential barriers in the quantum channel. A periodic multiwaveguide structure can be formed by cascading uniform waveguide sections of alternating widths, in which the narrow section is a constriction while the wide region between two constrictions is called a stub.<sup>11</sup> Studies of the transport properties of such structures have indicated that there exists a general ( $n-1$ )-fold resonant peak splitting for ballistic conductance when the structure consists of  $n$  constrictions.<sup>11,12</sup> The  $n-1$  peaks are induced by quasibound states whose wave functions are mainly confined in the stubs.<sup>11,12</sup> In analogy with the electric or magnetic superlattice, the stub in an open structure is usually regarded as a well while the constriction is a barrier. Accordingly, a periodic multiwaveguide structure consisting of  $n$  constrictions is usually regarded as an electric superlattice with  $n$  potential barriers. However, the constrictions in open periodic structures are not real potential barriers after all. In some cases, the electrons in the quantum states of open structure can be confined in the constrictions.<sup>15</sup> Thus the open periodic structure possesses some exotic transport properties different from those of the electric or magnetic superlattice.

In this paper, we first study the transport properties of a periodic multiwaveguide structure as shown in Fig. 1(a). It is interesting to find that there is ( $n-2$ )-fold resonant splitting at energies slightly higher than the first threshold energy, except for the ( $n-1$ )-fold resonant splitting in the lower-energy region of conductance. The origination of the ( $n-2$ )-fold splitting is analyzed using the quasibound states and effective mass picture. In the higher-energy region, the negative effective mass reverses the sign of the potential and thus each stub in the open structure acts as a potential barrier rather than a well. The  $n-2$  split peaks are induced by high quasibound states whose wave functions are mainly localized in the constrictions. The influence of the constriction length on the

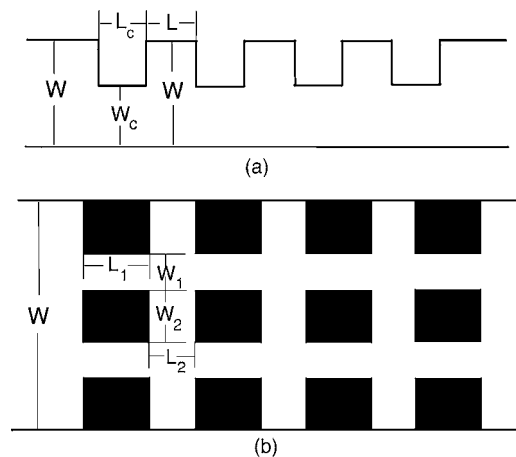


FIG. 1. (a) Schematic view of the periodic multiwaveguide structure, where a finite superlattice is connected to two leads with width  $W$ . The basic cell consists of a stub, with length  $L$  and width  $W$ , connected to a constriction of length  $L_c$  and width  $W_c$ . (b) Schematic view of the antidot arrays, where confined arrays are connected to two leads with width  $W$ . The length and width of the longitudinal constriction between two transverse antidots are  $L_1$  and  $W_1$ , respectively, while the length and width of the transverse constriction between two longitudinal antidots are  $L_2$  and  $W_2$ , respectively.

number of high quasibound states is discussed. Our calculations indicate that more quasibound states will exist in a constriction between two stubs as the constriction length increases. We also study the resonant splitting of a confined antidot array as shown in Fig. 1(b). Except for the resonant peaks obtained via the quasibound states localized in the junctions, the  $(n-2)$ -fold resonant splitting rule is found in the higher-energy region of conductance again. As in the case of the periodic multiwaveguide structure, the quasibound states corresponding to  $n-2$  resonant peaks are mainly localized in the constrictions of antidot arrays.

## II. MODEL AND METHOD

Let us consider two open periodic quantum structures as shown in Fig. 1. A periodic multiwaveguide structure is displayed in Fig. 1(a) where a finite superlattice is connected to two leads of width  $W$ . The finite superlattice consists of constrictions with size  $W_c \times L_c$  and stubs with size  $W \times L$ . While Fig. 1(b) shows finite-antidot arrays in confined geometries which are connected to two leads of width  $W$ . The antidots (black square areas) have been modeled by squarelike potential barriers with infinite height. The length and width of the longitudinal constriction between two transverse antidots are  $L_1$  and  $W_1$ , respectively, while the length and width of the transverse constriction between two longitudinal antidots are  $L_2$  and  $W_2$ . To calculate the transport properties of the two quantum structures, one can use the lattice Green's function (LGF) method.<sup>16-18</sup> In terms of the LGF scheme, the system is divided into a set of effective square lattices with lattice constant  $a$ . Hard wall boundaries are simply simulated by the absence of sites. To describe the electronic properties of the effective discretized system of a square lattice, one can define the tight-binding Hamiltonian<sup>16</sup>

$$H = \sum_{i,j} (\varepsilon_{i,j} + P_{i,j}) |i,j\rangle \langle i,j| + \sum_{i,j} V(|i,j\rangle \langle i,j+1| + \text{H.c.}) + \sum_{i,j} V(|i+1,j\rangle \langle i,j| + \text{H.c.}), \quad (1)$$

where  $\varepsilon_{i,j}$  is the site energy,  $P_{i,j}$  is the additional potential at the  $(i,j)$  site, and  $V$  is the hopping matrix element between the nearest-neighboring sites. Generally,  $\varepsilon_{i,j} = -4V$  and  $V = -\hbar^2/2m^*a^2$  ( $m^* = 0.067m_0$ ). We rewrite the Hamiltonian in units of the column cell as

$$H = \sum_i H_i + \sum_i (H_{i,i+1} + H_{i+1,i}), \quad (2)$$

where  $H_i$  is the Hamiltonian of the  $i$ th isolated column cell, and  $H_{i,i+1}$  and  $H_{i+1,i}$  are the intercell Hamiltonians between the  $i$ th and  $(i+1)$ th column cells with

$$H_{i+1,i} = \tilde{H}_{i,i+1}^*. \quad (3)$$

So the first two terms of Eq. (1) correspond to the first term of Eq. (2) and the last term of Eq. (1) corresponds to the second term of Eq. (2).

In terms of the definition of the Green's function  $\mathcal{G} = (E - H)^{-1}$  ( $E$  in units of  $-V$  is the electron energy), the Green's

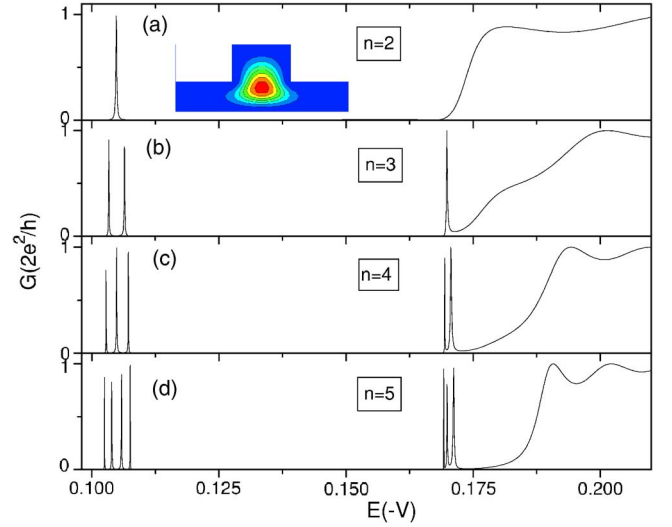


FIG. 2. (Color online) Conductance versus electron energy for a periodic multiwaveguide structure as shown in Fig. 1(a) with  $n$  constrictions.  $n =$  (a) 2, (b) 3, (c) 4, and (d) 5. Results are for the case  $W = 16a, L = 8a, W_c = 6a, L_c = 10a$ . Inset of (a): Contour plot of probability density of the quasibound state corresponding to the resonant peak in (a). The innermost contour curve represents the highest probability density and the contour curves in the two leads are not depicted.

function of each column and the Green's functions between two columns can be found. Using the recursive Green's function scheme,<sup>16,17</sup> one can obtain the Green's function of the system, which allows us to calculate the transmission coefficient  $T$  of the two-terminal system. Then conductance  $G$  is represented by the Landauer-Buttiker formula

$$G = \frac{2e^2}{h} T. \quad (4)$$

To calculate the eigenenergy  $E$  of a structure and the corresponding wave function  $\Psi$ , one can write the Hamiltonian of the system as

$$H = H_0 + \Sigma, \quad (5)$$

where  $H_0$  is the Hamiltonian of the structure without leads, and  $\Sigma$  is the total self-energy of the two leads. Solving the eigenequation  $H\Psi = E\Psi$ , one can obtain the eigenenergy  $E$  and wave function  $\Psi$ . In general, the eigenvalue is a complex whose imaginary part is associated with the lifetime of the eigenstate.<sup>18</sup>

## III. RESULTS AND DISCUSSION

In Fig. 2, we show the calculated conductance as a function of electron energy for a periodic multiwaveguide structure which includes  $n$  constrictions and  $n-1$  stubs. At the lower energies, one can see that  $n-1$  resonant peaks appear in the conductance profiles. These peaks are induced by low quasibound states. The inset in Fig. 2(a) displays the probability density of the quasibound state corresponding to the peak in Fig. 2(a). It is obvious that the electrons in the state

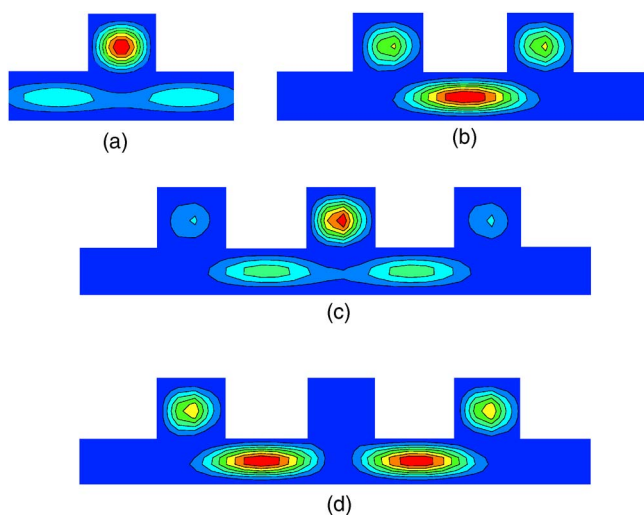


FIG. 3. (Color online) Contour plots of probability density of (a) the second eigenstate (eigenenergy  $E=0.17$ ) of the multiwaveguide structure with two constrictions, (b) the quasibound state corresponding to the third resonant peak in Fig. 2(b), (c) the quasibound state corresponding to the fourth resonant peak in Fig. 2(c), and (d) the quasibound state corresponding to the fifth resonant peak in Fig. 2(c).

are confined in the stub. As the structure consists of  $n$  constrictions, the coupling among the  $n-1$  lower quasibound states in the stubs generates  $(n-1)$ -fold split states. Accordingly,  $n-1$  split peaks from the split states appear in the conductance. For the low quasibound states, each stub is regarded as a well while each constriction is a barrier. Thus the periodic structure including  $n$  constrictions is equivalent to an electric superlattice with  $n$  potential barriers. However, at energies slightly higher than the first threshold energy, there are  $n-2$  resonant peaks in the conductance profiles. These peaks originate from the high quasibound states in the periodic structure. To explain this point, we first display in Fig. 3(a) the probability density of the second eigenstate (eigenenergy  $E=0.17$ ) of the simplest multiwaveguide structure with two constrictions, i.e.,  $n=2$ . In the longitudinal direction, it is found that the electrons in the eigenstate are mainly localized in the constrictions rather than in the stub. Due to the finite length of the constrictions, the eigenstate will couple with the continuum states in the lead; consequently the electrons in the eigenstate will escape to the lead. Our calculations also indicate that the lifetime of the state is very short, i.e., the eigenstate is not a quasibound state. Thus there is no resonant peak around  $E=0.17$  in Fig. 2(a). As the structure includes  $n=3$  constrictions, however, a high quasibound state will exist in the structure because of the coupling of the two adjacent eigenstates. Figure 3(b) shows the probability density of the quasibound state corresponding to the peak with energy  $E=0.17$  in Fig. 2(b). One can see that, in the longitudinal direction, the electrons in the state are mainly localized in the middle constriction rather than in the stubs. As the number of constrictions increases to  $n=4$ , the symmetric and antisymmetric superpositions of the two quasibound states, respectively localized in the two middle constrictions, generate two splitting states. The plots of probabil-

ity density of the two states corresponding to the fourth and the fifth split peaks in Fig. 2(c) are depicted in Figs. 3(c) and 3(d), respectively. With further increase of the period,  $n-2$  split peaks from the  $n-2$  high quasibound states will appear in the conductance profiles.

Compared with the low quasibound states confined in the stubs, the high quasibound states corresponding to the  $(n-2)$ -fold splitting are mainly localized in the constrictions. So the stubs of the high quasibound states are equivalent to potential barriers rather than wells, which is the inverse of the case of the low states. Why does the stub's effect change from well to barrier? This can be simply explained by the effective mass picture. Associated with Eq. (1), the Schrödinger equation for a discretized system is

$$\varepsilon_{i,j}\psi(x_i,y_j) + V[\psi(x_{i-1},y_j) + \psi(x_{i+1},y_j)] + V[\psi(x_i,y_{j-1}) + \psi(x_i,y_{j+1})] = E\psi(x_i,y_j), \quad (6)$$

where  $\psi(x_i,y_j)$  is the wave function at the  $(i,j)$  site. For a channel of constant width  $D=(m+1)a$  ( $m$  sites in the transverse direction), the wave function can be expressed as  $\psi(x,y) = \psi^{(k)}(x)\sin\frac{k\pi y}{(m+1)a}$  ( $k$  represents the index of the subband). At the lowest point of the energy band (band minimum), the effective mass is positive and the longitudinal wave function  $\psi(x)$  varies smoothly from point to point, i.e., the envelope  $|\psi\rangle = \sum \psi(x_i)|i\rangle$ . Then, expanding  $\psi$  in a Taylor series, for the lowest subband  $k=1$ , Eq. (6) becomes

$$\left(\varepsilon_{i,j} - 4|V| + \frac{\pi^2|V|}{(m+1)^2} + \dots\right)\psi^{(1)}(x_i) - a^2|V|\psi''^{(1)}(x_i) = E\psi^{(1)}(x_i). \quad (7)$$

So it seems reasonable that a constriction (a decrease in  $m$ ) would act as a potential bump, while a stub would act as an attractive well. However, at the high-energy point (band maximum), due to the envelope satisfying  $|\psi\rangle = \sum \psi(x_i) \times (-1)^i|i\rangle$ , the approximate effective mass equation becomes

$$\left(\varepsilon_{i,j} + \frac{\pi^2|V|}{(m+1)^2} + \dots\right)\psi^{(1)}(x_i) + a^2|V|\psi''^{(1)}(x_i) = E\psi^{(1)}(x_i). \quad (8)$$

This indicates that the longitudinal effective mass is negative, which essentially reverses the sign of the potential, including both  $\varepsilon_{i,j}$  and the pseudopotential term due to the transverse motion. Hence the constrictions become attractive wells while the stubs become repulsive barriers. In this case, an open periodic structure consisting of  $n-1$  stubs ( $n$  constrictions) is equivalent to an electric superlattice consisting of  $n-1$  potential barriers. This is the reason why  $(n-2)$ -fold resonant splitting appears in the high-energy region of the conductance.

In Fig. 4(a), the conductance as a function of electron energy for the structure in the inset is calculated. The structure includes two stubs and three constrictions. We discuss the effect of the length  $L_{cm}$  of the middle constriction on the high quasibound states in the constriction. The solid, dashed, and dotted lines, respectively, represent the conductance curves at  $L_{cm}=10a$ ,  $26a$ , and  $42a$ . One can see that the num-

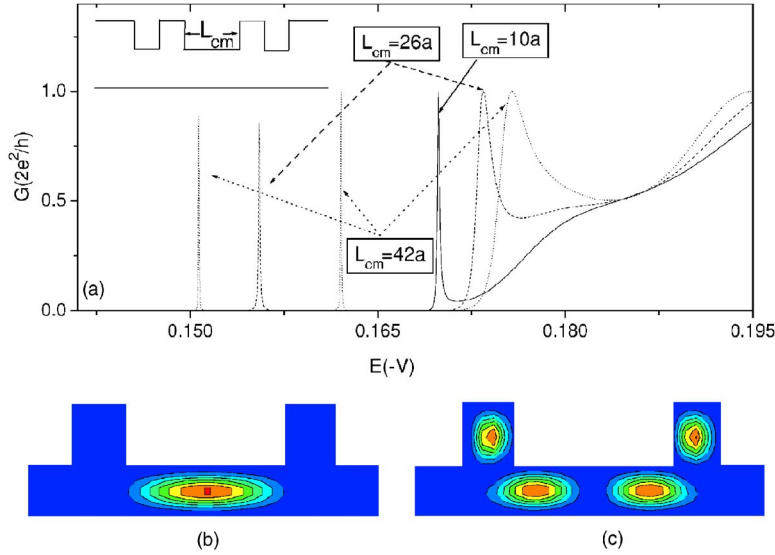


FIG. 4. (Color online) (a) Conductance versus electron energy for the structure in the inset with different lengths  $L_{cm}$  of the middle constriction. The solid, dashed, and dotted lines represent  $L_{cm}=10a$ ,  $26a$ , and  $42a$ , respectively. Other parameters are the same as in Fig. 2. Inset: Similar structure as in Fig. 1(a) with three constrictions; only the length of the middle constriction is represented by  $L_{cm}$ . (b), (c) Contour plots of the probability density of the quasibound states corresponding to the two peaks of the dashed line in (a): (b) the first and (c) the second resonant peak.

number of resonant peaks increases with the length, i.e., the number of high quasibound states in the constriction also increases with length. The electron probability densities of the two quasibound states corresponding to the two resonant peaks of the dashed line in Fig. 4(a) are shown, respectively, in Figs. 4(b) and 4(c). In the longitudinal direction, the two states are mainly localized in the middle constriction, and the wave functions of the two states are respectively even and odd symmetric with respect to the center line of the middle constriction. This is similar to the case of a quasi-one-dimensional double-barrier structure. It further indicates that, to the high quasibound states, the stubs are equivalent to potential barriers. Moreover, one expects that the quasibound states in the constrictions will disappear when the constriction length is short. Hence, in order to observe the  $(n-2)$ -fold splitting rule, the constrictions should be sufficiently long.

We then consider the resonant splitting in the conductance of a confined antidot arrays as shown in Fig. 1(b). In Fig. 5, the calculated conductance as a function of electron energy for an antidot arrays including 3 (row)  $\times$   $n$  (column) antidots is presented. As  $n=2$ , the structure includes two crossed junctions in the transverse direction. In each junction there exists a lower quasibound state. The transverse coupling between the two quasibound states in the junctions will lead to two split peaks in the lower-energy region of the conductance [see Fig. 5(a)]. With the periodic number increasing, each peak splits into  $n-1$  peaks. So there are  $2 \times (n-1)$  resonant peaks in the lower-energy region of the conductance curves in Fig. 5. These peaks correspond to  $2 \times (n-1)$  quasibound states whose wave functions are mainly localized in the crossed junctions. Except for peaks satisfying the  $(n-1)$ -fold splitting rule,  $(n-2)$ -fold split peaks appear in the higher-energy region around  $E=0.178$ . As in the case of the periodic multiwaveguide structure, these peaks are induced by higher-energy quasibound states in which electrons are mainly localized in the constrictions rather than in the junctions. Figure 6(a) displays the probability density of the quasibound state corresponding to the resonant peak with energy  $E=0.178$  in Fig. 5(b). To this kind of high state, the constrictions are equivalent to wells rather than barriers. In addition,

in Fig. 5 one can see that some resonant peaks exist in the conductance curves around  $E=0.1524$ . The number of these peaks should be  $n-1$ . Figure 6(b) shows the electron probability density of the quasibound state corresponding to the third peak in Fig. 5(a). It is found that the wave function of the quasibound state is tightly localized in the transverse constrictions. As the structure includes more periods, the longitudinal coupling between these states becomes very weak. Thus the energy difference of the split states is very small, and consequently the number of peaks induced by these states becomes uncountable.

#### IV. CONCLUSIONS

Using the LGF method, we calculated the conductance of two typical open periodic structures. For a periodic multiwaveguide structure including  $n$  constrictions,  $(n-1)$ -fold

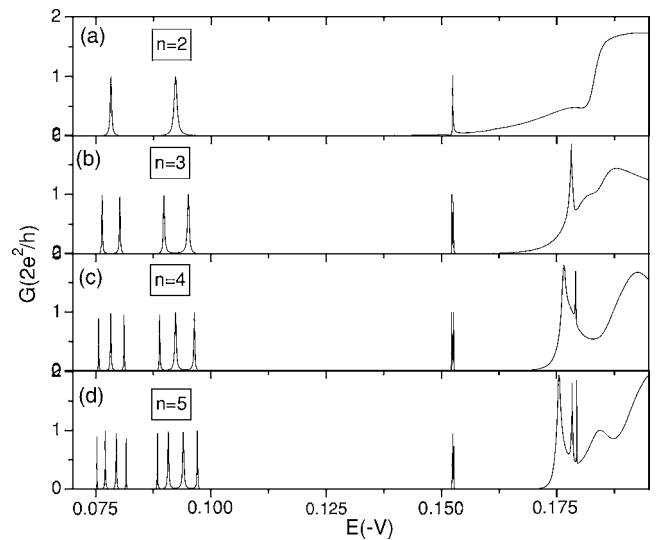


FIG. 5. Conductance versus electron energy for an antidot arrays as shown in Fig. 1(b) including 3 (row)  $\times$   $n$  (column) antidots.  $n=$  (a) 2, (b) 3, (c) 4, and (d) 5. Results are for the case  $L_1=10a$ ,  $W_1=6a$ ,  $L_2=8a$ ,  $W_2=10a$ ,  $W=42a$ .

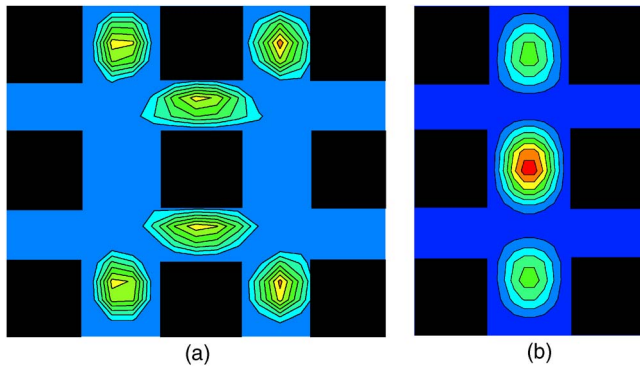


FIG. 6. (Color online) Contour plots of probability density of the quasibound states corresponding to (a) the resonant peak with  $E=0.1782$  in Fig. 5(b), (b) the resonant peak with  $E=0.1524$  in Fig. 5(a). The black square areas represent antidots.

split peaks appear at low energies of conductance while (*n*-2)-fold split peaks appear at high energies. The former resonant peaks are induced by quasibound states mainly localized in the stubs, while the latter peaks originate from

high quasibound states mainly localized in the constrictions. To the high quasibound states, the stubs act as potential barriers rather than wells, which is explained by the effective mass picture. More quasibound states will exist in the constriction between two stubs as the length of the constriction increases. For a periodic antidot arrays including 3 (row)  $\times$  *n* (column) antidots,  $2 \times (n-1)$  resonant peaks are found in the lower-energy region of the conductance. As in the case of the periodic multiwaveguide structure, the (*n*-2)-fold splitting rule exists around the first threshold energy. The quasibound states corresponding to *n*-2 peaks are mainly localized in the constrictions of the antidot arrays. In addition, quasibound states tightly localized in the transverse constrictions are also found.

**ACKNOWLEDGMENTS**

This work was supported by the Scientific Research Fund of Hunan Provincial Education Department (Grant No. 05C103) and Major Project of State Ministry of China (Grant No. 204099).

<sup>1</sup>R. Tsu and L. Esaki, Appl. Phys. Lett. **22**, 562 (1973); L. L. Chang, L. Esaki, W. E. Howard, and R. Ludeke, J. Vac. Sci. Technol. **10**, 11 (1973).  
<sup>2</sup>H. A. Carmona, A. K. Geim, A. Nogaret, P. C. Main, T. J. Foster, M. Henini, S. P. Beaumont, and M. G. Blamire, Phys. Rev. Lett. **74**, 3009 (1995).  
<sup>3</sup>R. Akis, P. Vasilopoulos, and P. Debray, Phys. Rev. B **56**, 9594 (1997).  
<sup>4</sup>J. E. F. Frost, I. M. Castleton, C. T. Liang, M. Pepper, D. A. Ritchie, E. H. Linfield, C. J. B. Ford, C. G. Smith, and G. A. C. Jones, Phys. Rev. B **49**, 14078 (1994).  
<sup>5</sup>R. Schuster, K. Ensslin, D. Wharam, S. Kuhn, J. P. Kotthaus, G. Bohm, W. Klein, G. Trankle, and G. Weimann, Phys. Rev. B **49**, 8510 (1994).  
<sup>6</sup>C. H. Kuan, D. C. Tsui, and K. K. Choi, Appl. Phys. Lett. **61**, 456 (1992).  
<sup>7</sup>Xue-Wen Liu and A. P. Stamp, Phys. Rev. B **47**, 16605 (1993).

<sup>8</sup>M. O. Vassell, J. Lee, and H. F. Lockwood, J. Appl. Phys. **54**, 5206 (1983).  
<sup>9</sup>F. M. Peeters and A. Matulis, Phys. Rev. B **48**, 15166 (1993).  
<sup>10</sup>Z. Y. Zeng, L. D. Zhang, X. H. Yan, and J. Q. You, Phys. Rev. B **60**, 1515 (1999).  
<sup>11</sup>K. Nikolic and R. Sordan, Phys. Rev. B **58**, 9631 (1998).  
<sup>12</sup>J. A. Brum, Phys. Rev. B **43**, 12082 (1991).  
<sup>13</sup>P. S. Deo and A. M. Jayannavar, Phys. Rev. B **50**, 11629 (1994).  
<sup>14</sup>Zhi-an Shao, Wolfgang Porod, and Craig S. Lent, Phys. Rev. B **49**, 7453 (1994).  
<sup>15</sup>Yuan Ping Chen, Yue E Xie, and Xiao Hong Yan, Eur. Phys. J. B **49**, 333 (2006).  
<sup>16</sup>Fernando Sols, M. Macucci, U. Ravaioli, and Karl Hess, Appl. Phys. Lett. **54**, 350 (1989); J. Appl. Phys. **66**, 3892 (1989).  
<sup>17</sup>T. Ando, Phys. Rev. B **44**, 8017 (1991).  
<sup>18</sup>Yuan Ping Chen, Xiao Hong Yan, and Yue E. Xie, Phys. Rev. B **71**, 245335 (2005).